⌘ *Author's Choice*

Negative Regulation of TGFβ Signaling by the Kinase LKB1 and the Scaffolding Protein LIP1*□S

Anita Morén[‡1], **Erna Raja**[‡1,2], **Carl-Henrik Heldin**[‡], **and Aristidis Moustakas**[‡§3]

From the ‡*Ludwig Institute for Cancer Research, Uppsala University, Box 595, Biomedical Center, Uppsala University, SE-751 24 Uppsala, Sweden and the* §*Department of Medical Biochemistry and Microbiology, Uppsala University, Box 582, Biomedical Center, Uppsala University, SE-751 23 Uppsala, Sweden*

Signal transduction by the Smad pathway elicits critical biological responses to many extracellular polypeptide factors, including TGFβ and bone morphogenetic protein. Regulation of Smad signaling imparts several cytoplasmic and nuclear mechanisms, some of which entail protein phosphorylation. Previous work established a protein complex between Smad4 and the scaffolding protein LKB1-interacting protein 1 (LIP1). LKB1 is a well studied tumor suppressor kinase that regulates cell growth and polarity. Here, we analyzed the LKB1-LIP1 and the Smad4-LIP1 protein complexes and found that LIP1 can self-oligomerize. We further demonstrate that LKB1 is capable of phosphorylating Smad4 on Thr[77] of its DNA-binding domain. LKB1 inhibits Smad4 from binding to either TGFβ- or bone morphogenetic protein-specific promoter sequences, which correlates with the negative regulatory effect LKB1 exerts on Smad4-dependent transcription. Accordingly, LKB1 negatively regulates TGFβ gene responses and epithelial-mesenchymal transition. Thus, LKB1 and LIP1 provide negative control of TGFβ signaling.

TGFβ and related polypeptides, such as bone morphogenetic proteins (BMPs),[4] signal via serine/threonine kinase receptors; upon ligand binding, a type II receptor phosphorylates a type I receptor to activate its kinase activity (1). Then the type I receptor phosphorylates cytoplasmic Smad proteins that constitute a small, conserved family of signal transducers. Upon phosphorylation, receptor-activated Smads (R-Smads) oligomerize with the common mediator Smad (Smad4), promoting binding to DNA and to cooperating transcription factors to regulate transcription. The inhibitory Smads form a negative feedback loop as their expression is induced by TGFβ/BMP Smad pathways, and their function inhibits receptor activity and promotes receptor down-regulation (2, 3).

TGFβ suppresses growth of many cell types because Smads and alternative signaling factors together induce expression of genes that enforce cell cycle arrest or apoptosis (4). In human cancers, some TGFβ signaling components (*e.g.* Smad4) become inactivated by mutation and free the tumor cell from the cytostatic constraints of this pathway (4). TGFβ also regulates epithelial cell polarity and differentiation by inducing epithelial-mesenchymal transition (EMT), which produces mesenchymal, migratory cells that support processes of normal tissue generation, wound healing, and cancer metastasis (5). During TGFβ-induced EMT, epithelial cell polarity is altered, leading to loss of adherens and tight junctions and of desmosomes, thus permitting the dissociation of cells from well organized epithelia (6).

Another important regulator of epithelial polarity is the tumor suppressor kinase LKB1 (liver kinase B1) (7). LKB1 has weak catalytic activity on its own and forms ternary complexes with the pseudokinase STRADα and the adaptor protein MO25α to create the catalytically active kinase (8). MO25α bridges STRADα with LKB1 and also induces an allosteric switch in STRADα that enhances the catalytic activity of LKB1 in the ternary complex (9). LKB1 phosphorylates and activates the catalytic activity of several members of the AMP-regulated protein kinase (AMPK) family, among which are the microtubule affinity-regulating kinases (MARKs) that regulate cell polarity (10). MARKs promote assembly of the polarity complex and epithelial polarization, resulting in the generation of tight and gap junctions (11). A screen for novel LKB1-interacting proteins using the yeast two-hybrid system uncovered the cytoplasmic scaffolding protein LIP1 (LKB1-interacting protein 1), which may tether LKB1 in the cytoplasm and which was shown to form complexes with Smad4 (12). Thus, LIP1 may provide a functional link between LKB1 and TGFβ/BMP Smad-dependent signaling.

LKB1 also activates another AMPK member, salt-inducible kinase (SIK), whose expression is transcriptionally induced in the adrenal glands of rats fed with a high salt diet (7, 13). SIK mRNA expression is also rapidly induced by TGFβ and BMP signaling, which leads to negative regulation of the TGFβ type I receptor in a mechanism that depends on the inhibitory Smad7 (14). Thus, SIK signaling can negatively regulate the TGFβ pathway. On the other hand, LKB1 can also induce

---

⌘ *Author's Choice*—Final version full access.

□S The on-line version of this article (available at http://www.jbc.org) contains supplemental Figs. S1–S3.

[1] Both authors contributed equally to this work.
[2] Supported by the Marie Curie Research Training Network "EpiPlastCarcinoma" under the European Union FP6 program (Project MRTN-2005-005428).
[3] To whom correspondence should be addressed. Tel.: 46-18-160411; Fax: 46-18-160420; E-mail: aris.moustakas@licr.uu.se.
[4] The abbreviations used are: BMP, bone morphogenetic protein; AMPK, AMP-regulated protein kinase; BRE, BMP-responsive element; EMT, epithelial-mesenchymal transition; LSM, LKB1, STRADα, MO25α complex; MARK, microtubule affinity-regulating kinase; SBE, Smad-binding element; R-Smad, receptor-activated Smad; SIK, salt-inducible kinase; TRITC, tetramethylrhodamine isothiocyanate.

expression of TGFβ ligand from mesenchymal cells, which then acts on neighboring epithelial cells in the gastrointestinal tract and limits their proliferation (15). This intercellular cross-talk between mesenchymal LKB1 and TGFβ signaling in neighboring epithelial cells explains the development of spontaneous gastrointestinal polyps generated by loss-of-function mutation of the *LKB1* gene in genetically modified mice or in humans exhibiting the familial Peutz-Jeghers syndrome (15). Loss of Lkb1 in murine mesenchymal cells also leads to decreased differentiation of myofibroblasts due to reduced TGFβ secretion (16). A similar mechanism explains why *Lkb1* knock-out mice die at midgestation from vascular defects because loss of Lkb1 function in endothelial cells reduces the amount of secreted TGFβ ligand, thus limiting the proper recruitment of vascular smooth muscle cells to the developing endothelium and perturbing proper angiogenesis (17). It is therefore important to explain the cell context-dependent action of LKB1 as a positive or negative regulator of TGFβ signaling.

In this study, we took a biochemical approach aimed at examining the role of LKB1 in regulating Smad signaling downstream of TGFβ or BMP. We first found that LKB1 cannot make direct complexes with Smad4. We then showed that the scaffolding protein LIP1 can oligomerize with itself. This result allows us to propose a model where LKB1 may contact Smad4 indirectly via the LIP1 oligomer. We also show that the functional LKB1 kinase complex of LKB1, STRADα, and MO25α (LSM), has the capacity to phosphorylate Smad4 on Thr[77] of its DNA-binding domain. LKB1 inhibits at least partially the direct binding of Smad4 to DNA and consequently negatively regulates the transcriptional activity of Smad4. This is confirmed by demonstrating that LKB1 inhibits the transcriptional regulation of various well established gene targets of TGFβ signaling, including markers of the EMT process. We therefore establish LKB1 as a negative regulator of TGFβ signaling and of the EMT response.

EXPERIMENTAL PROCEDURES

Cell Culture, Transfection, and Adenoviral Infection—Human embryonic kidney 293-T cells, human hepatoma HepG2 cells, human immortalized HaCaT keratinocytes, human breast cancer MDA-MB-468 and MDA-MB-231 cells, mouse NMuMG cells, clone NM18, and mouse pluripotent C2C12 cells were cultured in DMEM from Sigma-Aldrich, supplemented with 10% FBS. The human fibrosarcoma cell line HT-1080 that was stably transfected with the TGFβ/Smad-responsive promoter-reporter pCAGA$_{12}$-MLP-luc construct was a gift from S. Souchelnytskyi (Karolinska Institute, Stockholm) and was cultured in the same medium as described above in the presence of 0.7 μg/ml G418 (Invitrogen). Transient transfections of cells were done using calcium phosphate (18), Lipofectamine (Invitrogen), or Fugene HD (Roche Applied Science) according to standard protocols. Transient adenoviral infections of MDA-MB-468, C2C12, HaCaT, and NMuMG cells were performed as described previously (19), except that cells were starved in DMEM supplemented with 1% FBS prior to adenoviral infection. Cells were infected for 18–24 h prior to stimulations with TGFβ1 (5 ng/ml) or BMP7

(30 ng/ml) in DMEM with 1% FBS. For EMT assays, the cells were stimulated with TGFβ1 in DMEM with 10% FBS for 24–48 h. The adenoviruses for mouse Lkb1, human STRADα, and human MO25α were gifts from J. R. B. Dyck (20). Other adenoviruses used were adGFP, adLacZ, adCAGA$_9$, and adSmad4, which have been described before (19).

Plasmids and Other Reagents—The mammalian expression vectors pCDNA3 empty, pCDNA3-FLAG-Smad4, pCDNA3-caALK5-HA, and pCDNA3-caALK6-HA (also presented as pCDNA3-ALK6QD-HA) have been described (18). The human LIP1 (N-terminally tagged with FLAG or Myc epitopes) and LKB1 (N-terminally tagged with the Myc epitope) plasmids were a gift from A. Ashworth (12). MO25α and STRADα expression vectors were a gift from T. Mäkelä (16). pGEX vectors encoding GST-Smad4, GST-Smad4MH1, GST-Smad4MH2, and GST-Smad4ΔMH1 have been described (18, 21). Point mutations in the Smad4 MH1 construct were done using the QuikChange mutagenesis kit (Stratagene) with primers purchased from Sigma-Aldrich. The CAGA reporter pCAGA$_{12}$-MLP-luc, the BMP-responsive element (BRE)-luc reporter (BRE)$_2$-luc, and pCMV-β-gal used for normalization of transfection efficiency have been described before (18). The pRS empty vector and pRS-LIP1 shRNA vectors were derived from a genome-wide shRNA library provided by R. Bernards (22).

Recombinant mature TGFβ was bought from PeproTech EC Ltd. and BIOSOURCE Inc. The TGFβ1 isoform was used throughout this study. BMP7 was a gift from K. Sampath (Curis Inc.).

Antibodies—Rabbit polyclonal anti-LIP1 was raised in house by immunizing rabbits against a synthetic antigenic peptide (Cys-DRAKNSPPQAPSTRDHG), fused to the carrier protein keyhole limpet hemocyanin. The aspartic acid after the first cysteine on this peptide maps at position 767 of the human LIP1 protein. Mouse monoclonal anti-FLAG (M2 and M5) antibodies and anti-fibronectin (F3648) were from Sigma-Aldrich; mouse monoclonal anti-Myc (9E10 clone) and mouse monoclonal anti-HA (12CA5 clone) were produced in house from hybridoma cell lines; mouse anti-E-cadherin was from BD Pharmingen; mouse anti-LKB1, goat anti-STRADα, rabbit polyclonal anti-Smad4, and mouse monoclonal anti-β-tubulin were from Santa Cruz Biotechnology, Inc. (Santa Cruz, CA); rabbit anti-AMPKα was from Cell Signaling Inc.; mouse anti-PAI1 was from BD Pharmingen/Transduction Laboratories; mouse anti-GAPDH was from Ambion; and rabbit anti-MO25α was from Epitomics.

Immunoblotting and Co-immunoprecipitation Assays—Total proteins from transfected and/or infected and ligand-stimulated 293-T, HepG2, HaCaT, C2C12, NMuMG, and MDA-MB-468 cells were extracted in lysis buffer (0.5% Triton X-100, 11.5 mM deoxycholic acid, 20 mM Tris-HCl, pH 7.4, 150 mM NaCl, 10 mM EDTA, and complete protease inhibitor mixture from Roche Applied Science) for 20 min on ice, and the insoluble pellet was removed after centrifugation at 13,000 rpm for 10 min at 4 °C. Protein concentration was determined with a Bradford assay (Bio-Rad) according to the manufacturer's protocol. Equal amounts of protein were sub-

jected to SDS-PAGE and immunoblotted as described previously (19). Immunoblots were analyzed either using x-ray films or using a digital scanning system (Fujifilm Intelligent Dark Box II with associated CCD camera LAS-1000) and the software AIDA (Fuji Inc.). The reported optical density of the protein bands on the immunoblots was quantified using the AIDA software on scanned immunoblot images from x-ray films.

For co-immunoprecipitation assays, 293-T cells were either transfected with various constructs and/or treated as explained in the figure legends or left intact for endogenous co-immunoprecipitation assays. Cell extracts were immunoprecipitated with anti-FLAG, anti-LKB1, or anti-LIP1 antibodies 48 h after transfection. For the endogenous LIP1-Smad4 co-immunoprecipitation, anti-LIP1 was incubated in the absence or presence of 20 μg/ml LIP1 antigenic peptide as competitor. After four washes with lysis buffer, the immunocomplexes were resolved by SDS-PAGE and immunoblotted with antibodies, as described in the figure legends.

In Vitro Phosphorylation Assays and Phosphopeptide Analysis—GST-Smad4 and GST-LIP1 purified from *Escherichia coli*, as described previously (21), were combined in an *in vitro* kinase reaction using as buffer 50 mM Tris, pH 7.4, 1 mM dithiothreitol, 10 mM $MgCl_2$, 100 μM ATP, 1 μCi of [^{32}P]ATP, and the activated complex of human LKB1-human STRADα-human MO25α (Upstate) at 30 °C for 30 min. Reactions were washed once with reaction buffer and stopped by the addition of Laemmli buffer and subjected to SDS-PAGE. Gel processing and fujifilm (FLA-3000)-assisted visualization of radioactive proteins were performed as described before (21). The phosphopeptide analysis and Edman degradation were performed as described (23).

Electrophoretic Mobility Shift Assays (EMSAs)—For EMSAs, the following double-stranded oligonucleotides were produced (Sigma-Aldrich). The Smad3 or Smad4-binding oligonucleotide 4× CAGA was as follows: forward strand, 5′-CAGACAGTCAGACAGTCAGACAGTCAGACAGT-3′; reverse strand, 5′-ACTGTCTGACTGTCTGACTGTCT-GACTGTCTG-3′. The Smad1- and Smad4-binding oligonucleotide BRE from the mouse *Id1* enhancer was as follows: sense, 5′-CTAGCTCAGACCGTTAGACGCCAG-GACGGGCTGTCAGGCTGGCGCCTTTT-3′; antisense, 5′-AAAAGGCGCCAGCCTGACAGCCCGTCCT-GGCGTCTAACGGTCTGAGCTAG-3′. Semipurified recombinant GST-Smad4MH1 WT and GST-Smad4MH1 T77A mutant proteins were incubated with the radiolabeled DNA probes, and the EMSA was performed as described before (24).

Chromatin Immunoprecipitation (ChIP) Assays—HaCaT cells were grown to 70–80% confluence in 10-cm plates and stimulated with 5 ng/ml TGFβ1 for 1.5 h, prior to cross-linking with 1% formaldehyde via incubation on a shaking platform for 10 min at room temperature. Cross-linked cells were washed with ice-cold PBS, and cell pellets were resuspended in 1 ml of lysis buffer (50 mM Tris-HCl, pH 8.0, 10 mM EDTA, 1% SDS, supplemented with protease inhibitor mixture (Roche Applied Science)). Total cell lysate was sonicated in a water bath Diagenode Bioraptor sonicator with 30-s pulses for

15 min at high frequency to obtain short DNA fragments. The lysate was subsequently centrifuged at 14,000 rpm in 4 °C for 10 min. Afterward, chromatin immunoprecipitation was performed overnight at 4 °C with 5 μg of mouse monoclonal anti-Smad4 (Santa Cruz Biotechnology) or 5 μg of nonspecific preimmune mouse immunoglobulin (home-made), together with magnetic beads (Dynabeads M280 Invitrogen) and dilution buffer (20 mM Tris-HCl, pH 8.0, 2 mM EDTA, 1% Triton-X100, 150 mM NaCl, and protease inhibitor mixture (Roche Applied Science)) in a total volume of 9 ml (sonicated cell lysate was diluted 1:10). The precipitated complexes were washed five times with washing buffer (50 mM HEPES-KOH, pH 7.0, 0.5 M LiCl, 1 mM EDTA, 0.7% (w/v) deoxycholate, 1% Igepal CA630) and once with TE buffer (10 mM Tris-HCl, pH 8.0, 1 mM EDTA). DNA was eluted in 200 μl of elution buffer (lysis buffer without protease inhibitor mixture) after shaking at 65 °C for 6 h. For the ChIP input controls, 100 μl of sonicated cell lysate was diluted 4 times with elution buffer and treated at 65 °C for 6 h as well. Eluted DNA and input DNA were purified using a PCR purification kit (Qiagen) and then analyzed by a quantitative PCR assay using specific primers for the human *PAI-1* (plasminogen activator inhibitor 1) gene: forward, 5′-GCAGGACATCCGGGAGAGA-3′; reverse, 5′-CCAATAGCCTTGGCCTGAGA-3′. The quantitative PCR protocol was as follows: 95 °C for 5 min, followed by 39 cycles of 95 °C for 15 s and 60 °C for 1 min.

Phase-contrast and Immunofluorescence Microscopy—Phase-contrast microscopy of NMuMG cells was performed using an Axiovert 40 CFL Zeiss microscope and an AxioCam MRc CCD camera. HaCaT cells were analyzed by immunofluorescence as described previously (19). Fibronectin primary antibody was described above, and TRITC-labeled phalloidin (Sigma-Aldrich) was used to stain the actin cytoskeleton. The secondary antibody used for immunofluorescence was Alexa fluor 546-conjugated goat anti-rabbit-IgG (Invitrogen). Nuclei were counterstained with DAPI (Sigma-Aldrich). Primary images were acquired with the microscope's CCD camera, image memory content was reduced, and brightness-contrast was adjusted using Adobe Photoshop 6.0.

Breast Cancer Cell Invasion Assays—MDA-MB-231 cells were first infected with adenoviral vectors as described above. After 24 h, $1 × 10^5$ infected cells were seeded into a Matrigel-coated transwell system (BD Biosciences) and were treated with vehicle or 5 ng/ml TGFβ1 for 24 h. Cells invading into the matrix and migrating to the bottom side of the well were stained with Wright-Giemsa and counted manually under an Axiovert 40 CFL Zeiss microscope.

Transfections with siRNA Oligonucleotides—C2C12 cells were treated with 20 nM siRNA oligonucleotides targeting mouse *Lkb1/Stk11* (Dharmacon ON-TARGETplus SMART pool L-044342–00) or 20 nM non-targeting control (Dharmacon ON-TARGETplus Non-targeting pool D-001810-10). NMuMG cells were treated with a 10 nM concentration of the same siRNAs. HaCaT cells were treated with 10 nM human si*LKB1/STK11* (Dharmacon ON-TARGETplus SMART pool L-005035-00) or 10 nM non-targeting control siRNA as described above. HT-1080/CAGA-luc cells were treated with 10 nM human si*LIP1/STK11IP* (Dharmacon ON-TARGETplus

Negative Regulation of TGFβ Signaling by LKB1

SMART pool L-015159-00) or 10 nM non-targeting control siRNA as described above. The transfections in all cell lines were done using SilentFect from Bio-Rad in DMEM with 10% FBS for 24 h, and 48 h after transfection, cells were starved in DMEM with 1% FBS for 18–24 h prior to stimulation with TGFβ1 or BMP7. For EMT assays, HaCaT or NMuMG cells were stimulated with TGFβ1 in DMEM with 10% FBS 2 days after siRNA transfection.

Luciferase Assays—HepG2, HaCaT, and 293-T cells were transiently transfected with the TGFβ/Smad-responsive promoter-reporter pCAGA$_{12}$-MLP-luc construct or the BMP/ Smad-responsive construct pBRE$_2$-luc for 36 h prior to stimulation with TGFβ1 or BMP7 for 16 h. pCMV-β-gal was transfected as a control for normalization. Additional constructs were included in the transfections according to the figure legends. Luciferase reporter assays were performed with the enhanced luciferase assay kit from BD PharMingen, Inc., according to the protocol of the manufacturer. Normalized promoter activity data are plotted in bar graphs that represent average values from triplicate determinations with S.D. values. Each independent experiment was repeated at least twice.

HaCaT and C2C12 cells were also infected with adCAGA$_9$-luc and adLacZ as a control before stimulation with TGFβ1. The cells were lysed in lysis buffer containing 5 mM sodium phosphate buffer, pH 7.8, 2 mM dithiothreitol, 2 mM CDTA (*trans*-1,2-diaminocyclohexane-*N*,*N*,*N*′,*N*′-tetraacetic acid), 10% glycerol, and 1% Triton X-100. The luciferase reporter assay was performed as described above. The β-galactosidase assay was performed by mixing the cell lysate with 100 mM sodium phosphate, pH 7.3, 1 mM MgCl$_2$, 50 mM β-mercaptoethanol, and 0.67 mg/ml ONPG (2-nitrophenyl β-D-galactopyranoside); the absorbance was read at 420 nm after incubation at 37 °C.

Real-time RT-PCR—RNA was extracted using the RNeasy kit from Qiagen. cDNA was subsequently synthesized using the iScript cDNA synthesis kit from Bio-Rad. Real-time RT-PCR was done using iTaq SYBR green supermix from Bio-Rad. The gene-specific primers used are as follows: mouse *Lkb1*, 5′-GCCTCCTGAGATTGCCAATG-3′ (forward) and 5′-GGTACAGGCCCGTGGTGAT-3′ (reverse); human *STRADα*, 5′-TTCCAATGAGATGGTAACAT-TCTTG-3′ (forward) and 5′-GCACGATATTGGGATGGTT-GA-3′ (reverse); human *MO25α*, 5′-GAGAGCATGGCTGT-TCTGGAA-3′ (forward) and 5′-ACCAGATTTTTGGAAAC-TTCTTCTG-3′ (reverse); mouse *Pai1*, 5′-GGCAGATCCAA-GATGCTATGG-3′ (forward) and 5′-TCATTCTTGTTCCA-CGGCC-3′ (reverse); mouse E-cadherin, 5′-GACTGTGAAG-GGACGGTCAAC-3′ (forward) and 5′-CCACCGTTCTCCT-CCGTAG-3′ (reverse); mouse fibronectin, 5′-CCCAGACTT-ATGGTGGCAATTC-3′ (forward) and 5′-AATTTCCGCCT-CGAGTCTGA-3′ (reverse); mouse *Snail1*, 5′- CCACTGCA-ACCGTGCTTTT-3′ (forward) and 5′-CACATCCGAGTGG-GTTTGG-3′ (reverse); mouse *Slug*, 5′-CGGGAGCATACAG-CCCTATTACT-3′ (forward) and 5′-GGCCACTGGGTAAA-GGAGAGT-3′ (reverse); human *ID1*, 5′-GGACGAGCAGC-AGGTAAACG-3′ (forward) and 5′-TGCTCACCTTGCGG-TTCTG-3′ (reverse); human *GAPDH*, 5′-GGAGTCAACGG-ATTTGGTCGTA-3′ (forward) and 5′-GGCAACAATATCC-ACTTTACCA-3′ (reverse); mouse *gapdh*, 5′-TGTGTCCGT-CGTGGATCTGA-3′ (forward) and 5′-CCTGCTTCACCAC-CTTCTTGA-3′ (reverse).

RESULTS

LIP1 Forms Complexes with LKB1 and Smad4 and Self-oligomerizes—Based on our recent demonstration that SIK, one of the kinases acting downstream of LKB1, negatively regulates TGFβ receptor signaling (14), we investigated directly the role of LKB1 as a regulator of the TGFβ pathway. A link between LKB1 and TGFβ family pathways via the scaffolding protein LIP1, which can interact with LKB1 and Smad4, has been suggested (12).

In order to study the protein complexes formed between LKB1, LIP1, and Smad4, we generated a rabbit polyclonal antibody that recognizes human LIP1 (see "Experimental Procedures"). This antibody was raised against a peptide that maps on the C-terminal third of the 1,099-amino acid residue-long LIP1 protein. Co-immunoprecipitation assays using this antibody and all three proteins transfected in 293-T cells indicated the formation of complexes between the transfected LKB1, LIP1, and Smad4, with traces of endogenous LKB1 observed in the LIP1 co-precipitates (Fig. 1*A*, *lane 1*). In the same experiments, endogenous LIP1 could co-precipitate transfected Smad4 or transfected LKB1, again with traces of endogenous LKB1 also being detectable in the co-precipitates (Fig. 1*A*, *lanes 2* and *3*). In addition, LIP1 formed strong complexes with LKB1 alone or Smad4 alone (Fig. 1*A*, *lanes 4* and *5*). Co-immunoprecipitation assays using an antibody against LKB1 revealed strong complexes between transfected LIP1 and LKB1 and much weaker participation of transfected Smad4 in these complexes (Fig. 1*B*, *lanes 1–3*). In these assays, endogenous LKB1 also co-precipitated weaker but detectable levels of transfected LIP1 (Fig. 1*B*, *lane 4*). Co-immunoprecipitation assays using an antibody against transfected F-Smad4 (FLAG) failed to detect endogenous LKB1 (Fig. 1*C*, *lane 1*) but readily detected the complex with transfected LIP1 (Fig. 1*C*, *lane 2*). When all three proteins were co-transfected, the same FLAG antibody co-precipitated less F-Smad4 and even less LIP1, whereas the transfected LKB1 remained again undetectable (Fig. 1*C*, *lane 3*). Repeated trials confirmed that only the LIP1 antibody could co-precipitate transfected Smad4 and LKB1 with traces of endogenous LKB1 (supplemental Fig. S1*A*).

We then repeated the experiment using an antibody that recognizes endogenous human Smad4 (Fig. 1*D*). Using the LIP1 antibody and the corresponding peptide as a specific competitor, we could verify the presence of an endogenous complex between LIP1 and Smad4 in HaCaT cells (Fig. 1*D*). The competitor peptide effectively blocked the ability of the LIP1 antibody to pull down Smad4, suggesting that this was a genuine co-immunoprecipitation and not a nonspecific pulldown of Smad4 by the polyclonal rabbit antiserum.

When LKB1 and Smad4 were overexpressed together, they could form detectable complexes that were sometimes weaker and sometimes stronger, depending on the level of LKB1 overexpression (Fig. 1, *B* (*lane 3*) and *E* (*lane 2*)). Knockdown
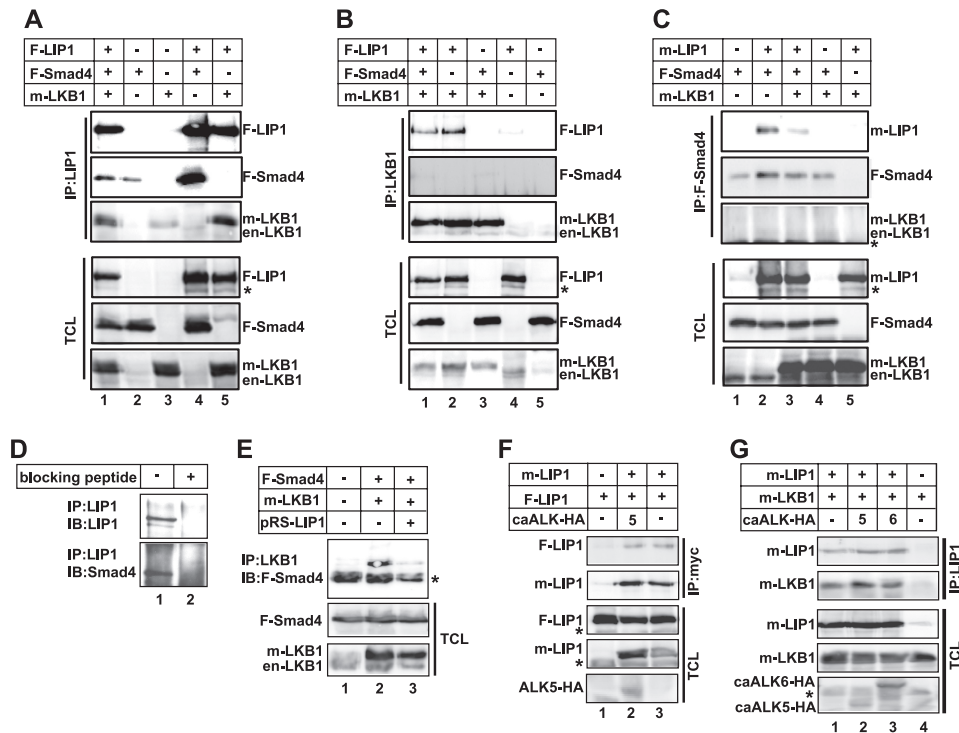
FIGURE 1. **LIP1 self-oligomerizes and forms complexes with LKB1 and Smad4.** *A*, co-immunoprecipitation (*IP*) assays using a LIP1-specific antibody and 293-T cell extracts from cells transfected with the indicated untagged, FLAG (*F*)-tagged or Myc (*m*)-tagged proteins. Immunoblotting of the immunocomplexes or input total cell lysates (*TCL*) with anti-FLAG or anti-LKB1 antibodies was then performed. *B*, same experimental design as in *A* except that co-immunoprecipitation was performed with anti-LKB1 antibody followed by immunoblot with anti-FLAG or anti-LKB1 antibodies. *C*, same experimental design as in *A* except that Myc-tagged LIP1 (*m-LIP1*) was transfected, and co-immunoprecipitation was performed with anti-FLAG antibody (*F-Smad4*) followed by immunoblot with anti-Myc, anti-FLAG, or anti-LKB1 antibodies. *D*, endogenous LIP1 co-immunoprecipitates with endogenous Smad4 in HaCaT cells. Incubation of the immunoprecipitates with the immunogenic anti-LIP1 peptide serves as specificity control. *E*, co-immunoprecipitation of LKB1 with FLAG-Smad4 in 293-T cells transfected with the indicated proteins and the shRNA-encoding vector pRS-LIP1. Immunoblotting (*IB*) with antibodies for the indicated proteins was then performed. *F*, co-immunoprecipitation assay between Myc-tagged LIP1 and FLAG-tagged LIP1 (*F-LIP1*) in the absence or presence of co-transfected HA-tagged constitutively active type I receptor caALK5. *G*, co-immunoprecipitation assay between Myc-tagged LIP1 and Myc-tagged LKB1 (*m-LKB1*) in the absence or presence of co-transfected HA-tagged constitutively active type I receptor caALK5 or caALK6. Co-immunoprecipitation was performed using the LIP1-specific antibody followed by anti-Myc immunoblotting. Total cell lysates show the expression levels of all transfected proteins. In all panels, *asterisks* show nonspecific protein bands; endogenous LKB1 is also marked (*en-LKB1*).

of endogenous LIP1 by transfecting a retroviral vector encoding a shRNA hairpin against human LIP1 dramatically reduced the efficiency of the LKB1-Smad4 protein complex (Fig. 1*E*, *lane 3*). This was the case despite the fact that this shRNA could only reduce the endogenous LIP1 levels to roughly 30–40% compared with the endogenous LIP1 levels in 293-T cells transfected with the control shRNA vector (supplemental Fig. S1*B*). The shRNA sequence used was able to knock down effectively transfected constructs of human LIP1 cDNA that contained the target sequence of the shRNA, which maps at the N-terminal part of the cDNA, whereas LIP1 constructs spanning the C-terminal part of LIP1 were not affected at all, as expected (supplemental Fig. S1*C*).

We then asked whether stimulation of signaling pathways in which Smad4 participates, namely TGFβ and BMP pathways, had any impact on the formation of the LIP1-LKB1-Smad4 complexes. In the course of these experiments, we first found that LIP1 was able to self-oligomerize (Fig. 1*F*, *lane 3*). Pathway stimulation mimicking TGFβ signaling by means of co-transfection of a constitutively active (ca) TGFβ type I receptor (caALK5; activin receptor-like 5), had no significant impact on LIP1 self-oligomerization (Fig. 1*F*, *lane 2*). Similar experiments using the same constitutively active TGFβ receptor or the constitutively active BMP type I receptor (caALK6)

failed to demonstrate any obvious effects on formation of the LIP1-LKB1 complexes (Fig. 1*G*) or on the LIP1-Smad4 complexes.[5] We therefore conclude that LIP1 most probably forms separate complexes with either Smad4 or LKB1.

LKB1 Phosphorylates Smad4 on Threonine 77—We explored the possibility that LKB1 phosphorylates LIP1 or Smad4 by using a recombinant LKB1 kinase together with its obligatory co-factors STRADα and MO25α that assemble the functionally relevant LKB1 kinase complex (8). In the absence of STRADα and MO25α, recombinant LKB1 was unable to perform efficiently *in vitro* phosphorylation reactions.[5] Inclusion of the pseudokinase STRADα and the adaptor protein MO25α and purification of the active LSM ternary complex were sufficient to observe robust *in vitro* phosphorylation events (Fig. 2 and supplemental Fig. S2). *In vitro* phosphorylation reactions with LSM complexes alone revealed phosphorylation of STRADα and MO25α in the trimeric protein complex (Fig. 2*A*). Furthermore, co-incubation of the LSM complex with bacterially purified GST-LIP1 as a substrate revealed that LKB1 is capable of phosphorylating the N-terminal half but not the C-terminal half of this protein
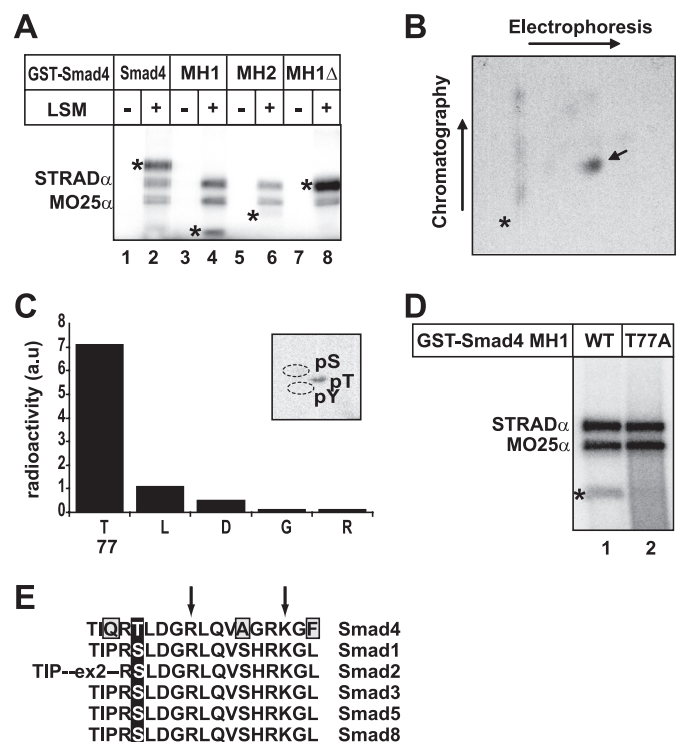

FIGURE 2. **LKB1 phosphorylates the MH1 domain of Smad4 at threonine 77.** *A*, *in vitro* kinase assay using recombinant LSM, [γ-^{32}P]ATP, and recombinant GST-Smad4 proteins as indicated. Autoradiography of the phosphorylated proteins was recorded using a fujifilm image. *Asterisks* indicate the positions of the Smad4 proteins. The phosphorylated STRADα and MO25α are also marked. *B*, two-dimensional electrophoresis coupled to chromatography of the tryptic fragments of the GST-Smad4 MH1 domain after *in vitro* kinase reaction with LSM as in *A*. The *arrows* on the *side* of the autoradiogram indicate the direction of migration of the proteins. An *asterisk* indicates the application point of the enzymatic digest on the silica plate. A *small arrow* indicates the major phosphopeptide recovered. *C*, diagram of the ^{32}P-counts (presented with arbitrary units (*a.u.*)) of radioamino acids produced after Edman degradation of the major phosphopeptide shown in *B*. Amino acids are shown on the *x* axis, and Thr^{77} is *marked* with its coordinate. The *inset* shows corresponding phosphoamino acid analysis in a chromatogram of an aliquot of the same phosphopeptide used for Edman degradation. The expected positions of phosphoserine and phosphotyrosine are shown with *dotted circles*. *D*, *in vitro* kinase assay as in *A* with WT and T77A Smad4 mutant MH1 domain as substrate. An *asterisk* indicates the position of the GST-Smad4 MH1 domain. *E*, sequence alignment of human Smad4 along the five human R-Smads. A *black box* highlights the phosphorylated Thr^{77}. *Gray boxes* indicate the only amino acid residue differences between Smad4 and the R-Smad sequences in this highly conserved segment of the proteins. *Arrows* indicate the amino acid residues that contact directly DNA on SBEs.

(supplemental Fig. S2*A*). Thus, LIP1 can be a potential target of phosphorylation by LKB1.

Repeating the *in vitro* phosphorylation assay with the LSM complex and bacterially purified GST-Smad4 also led to robust phosphorylation of Smad4 (Fig. 2*A*). Using Smad4 deletion constructs, we observed that LKB1 phosphorylated the N-terminal Mad homology 1 (MH1) domain of Smad4 or a mutant that carried the MH1 and linker domains but lacked the C-terminal MH2 domain (MH1Δ). Furthermore, LKB1 phosphorylated a Smad4 fragment composed only of the linker domain (supplemental Fig. S2*B*). In contrast, co-incubation with the purified MH2 domain did not lead to detectable phosphorylation (Fig. 2*A*). The latter construct also served as a specificity control, showing that a related protein domain fused to GST fails to be effectively phosphorylated by the

LSM kinase. Thus, LKB1 may phosphorylate Smad4 in two distinct domains, the N-terminal MH1 and linker domain. In addition to GST-Smad4, we could also observe reproducible phosphorylation of the Smad3 MH1 domain (supplemental Fig. S2*B*).

Tryptic digestion of the LKB1-phosphorylated MH1 domain of Smad4 resulted in a single major phosphopeptide and several weaker peptides (Fig. 2*B*). Phosphoamino acid analysis of the major phosphopeptide revealed phosphorylation of threonine but not of serine or tyrosine (Fig. 2*C*, *inset*). Edman degradation of the isolated phosphopeptide indicated phosphorylation of Thr^{77} in the MH1 domain of Smad4 (Fig. 2*C*). Site-specific mutagenesis of Thr^{77} to alanine abolished phosphorylation of the Smad4 MH1 domain by the LKB1 complex (Fig. 2*D* and supplemental Fig. S2*B*).

We therefore conclude that an active LKB1 kinase complex is capable of phosphorylating Thr^{77} in the N-terminal MH1 domain of Smad4. The analogous position is occupied by a serine residue in all of the R-Smads of the TGFβ family (Fig. 2*E*). Under physiological conditions within cells, it is therefore possible that active LKB1 kinase phosphorylates LIP1, Smad3, and Smad4.

LKB1 Inhibits the DNA Binding and Transcriptional Activity of Smad4—The position of Thr^{77} in the core of the MH1 domain of Smad4 immediately suggested that such phosphorylation might affect binding of Smad4 to its cognate Smadbinding element (SBE) sequence, 5′-CAGAC-3′. This threonine residue precedes by 4 and 11 residues Arg^{81} and Lys^{88}, the two critical amino acids of the β-hairpin of Smad4 that contact the SBE DNA and are critical for the transcriptional activity of this protein (24). We therefore performed EMSAs using recombinant GST-Smad4 MH1 domain because this domain exhibits robust DNA binding in the absence of a requirement for the R-Smads or cooperating transcription factors in the nuclear Smad complex (Fig. 3, *A* and *B*). Using this recombinant Smad4 domain, we could measure direct effects of LKB1-mediated phosphorylation on Smad4 DNA-binding, excluding indirect effects of LKB1 on any of the other cofactors of Smad4 required for assembly of the native DNA-bound nuclear Smad4 complex. Incubation of the recombinant Smad4 MH1 domain with the catalytically active LSM enzyme prior to the DNA binding reaction resulted in a significant decrease of the observed binding to the SBE or BRE probes (Fig. 3, *A* and *B*). The SBE probe contains four tandem copies of the SBE, whereas the BRE probe contains two SBE and two GC-rich sequences and represents a native sequence from the mouse *Id1* (inhibitor of differentiation 1) enhancer (27). The T77A mutant MH1 domain exhibited weaker but significant binding to the SBE and BRE DNAs presumably because mutation of an amino acid residue so close to the β-hairpin loop perturbs DNA binding (Fig. 3, *A* and *B*). Despite this, preincubation of the mutant T77A Smad4 domains with the LSM enzyme failed to demonstrate any further decrease of binding to the SBE or BRE DNA (Fig. 3, *A* and *B*). Thus, LKB1 decreases binding of Smad4 to DNA, presumably via phosphorylation of Thr^{77} of the DNA-binding domain of Smad4.
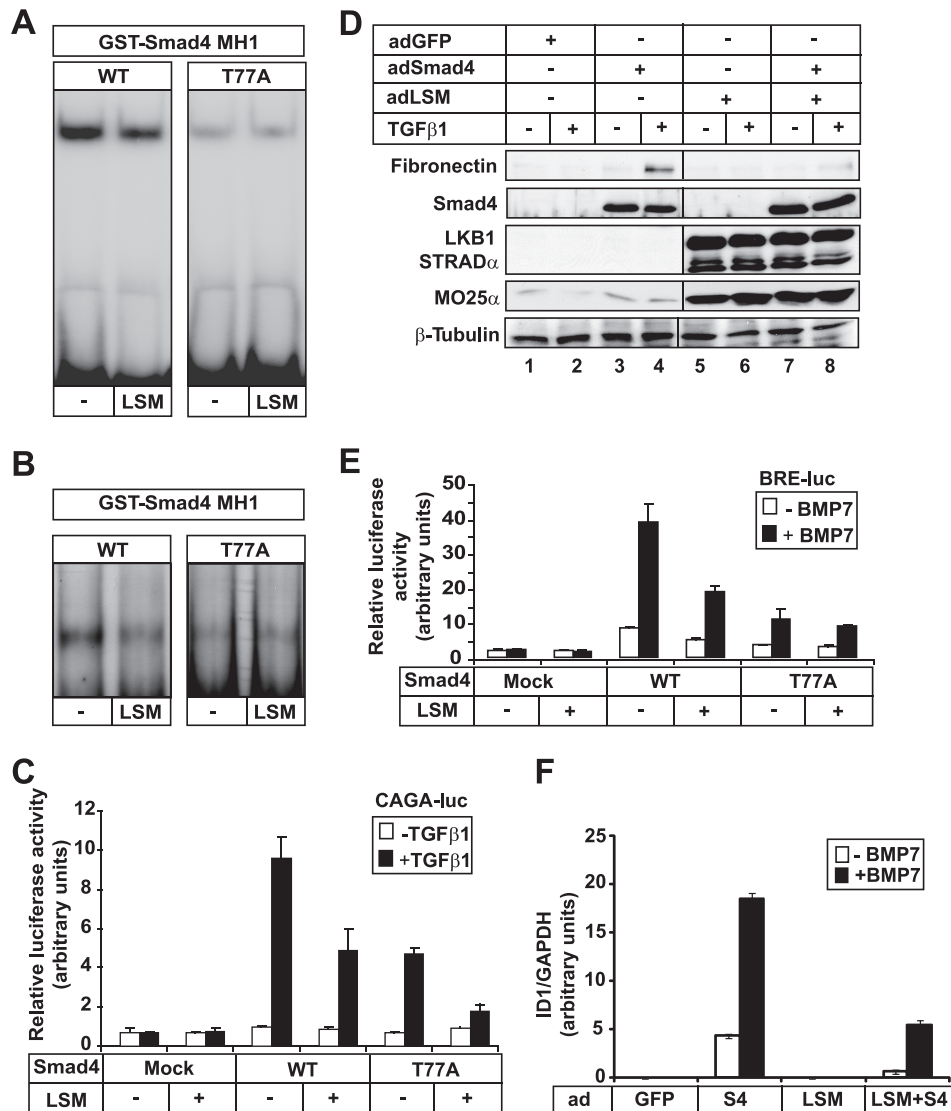
FIGURE 3. **LKB1 inhibits the DNA binding and the transcriptional activity of Smad4.** *A* and *B*, *in vitro* EMSA using recombinant WT or T77A mutant GST-Smad4 MH1 domain. Prior to the DNA binding reaction, the GST-Smad4 MH1 protein was incubated with *in vitro* kinase reaction buffer in the absence (−) or presence (+) of the LSM complex and cold ATP. The Smad3/Smad4-specific 4× CAGA oligonucleotide (*A*) or the Smad1/Smad4-specific BRE oligonucleotide (*B*) was incubated with the recombinant proteins. The autoradiograms show the input radiolabeled oligonucleotide (*bottom*) and the single protein bandshift observed (*top*). *C*, luciferase assay in MDA-MB-468 cells transiently transfected with the indicated DNA plasmids and stimulated or not with 5 ng/ml TGFβ1 for 16 h. The luciferase activity after normalization to the corresponding β-galactosidase activity was normalized to 1 in the condition of mock plasmid transfection. The *bar graph* shows average values derived from triplicate determinations and their corresponding S.D. values. Each transfection experiment was repeated at least twice. *D*, immunoblot of MDA-MB-468 cells transiently infected with the indicated adenoviral (*ad*) vectors and stimulated or not with 5 ng/ml TGFβ1 for 24 h as indicated. Endogenous fibronectin, endogenous β-tubulin as loading control, and the transduced levels of Smad4, STRADα, MO25α, and LKB1 are shown. The endogenous levels of STRADα and MO25a are too weak to be detected in these immunoblots. *E*, luciferase assay in MDA-MB-468 cells performed as in *C* except that the cells were transfected with the BRE-luc reporter and stimulated with 30 ng/ml BMP7 for 16 h. *F*, real-time RT-PCR analysis of endogenous *ID1* mRNA normalized to the corresponding *GAPDH* mRNA from MDA-MB-468 cells infected with the indicated adenoviral vectors and stimulated with 30 ng/ml BMP7 for 24 h. Average values from triplicate determinations and the corresponding S.D. values (*error bars*) are *graphed*.

Based on the latter result, we predicted that LKB1 should also negatively affect the functional output of Smad4-specific transcriptional reporters (Fig. 3C). CAGA-luc is a reporter that contains a 12-time concatamerized SBE sequence derived from the PAI-1 enhancer, to which Smad3 and Smad4 directly bind and induce robust transcription (28). In order to provide evidence for a direct involvement of Smad4 in the regulation of this promoter by TGFβ and LKB1 signaling, we made use of human breast carcinoma MDA-MB-468 cells, which lack the genomic locus of Smad4 and in which gene expression in response to TGFβ or BMP strictly depends on

reconstitution of wild-type Smad4 (19). In the absence of Smad4 transfection, the CAGA-luc reporter was silent, and the active LSM enzyme, provided by transfection of its three components, had no effect (Fig. 3C). Upon reconstitution of wild-type Smad4, we could observe robust activation of the reporter by TGFβ, and active LSM reduced this response (Fig. 3C), which is compatible with the decreased DNA binding of Smad4 caused by LSM (Fig. 3, *A* and *B*). As expected from the DNA-binding experiments, reconstitution of MDA-MB-468 cells with the Smad4 T77A mutant exhibited significant but weaker activation of the transcriptional reporter when com-

pared with the effect of wild-type Smad4 (Fig. 3*C*). Unexpectedly, co-expression of LSM together with the Smad4 T77A mutant further decreased the transcriptional output of the reporter, demonstrating that this mutant is not fully resistant to the action of LKB1 (Fig. 3*C*). This may be due to the ability of LKB1 to phosphorylate the linker of Smad4 (supplemental Fig. S2*B*). In a cellular context, therefore, LKB1 may regulate additional components of the nuclear Smad4 complex (*e.g.* Smad3, as demonstrated here) that have an impact on transcriptional activity.

In order to demonstrate that LKB1 can negatively regulate transcriptional events induced by TGFβ at the endogenous level, we employed again the Smad4-null MDA-MB-468 cells and adenovirus-mediated transfection of control (GFP) or Smad4 protein in the absence or presence of the three components of the LSM enzymatic complex (Fig. 3*D*). As a readout, we measured the synthesis of fibronectin protein, one of the well established gene targets of TGFβ. These assays also confirmed that fibronectin expression was induced only after reconstitution of wild-type Smad4, whereas co-expression of the LSM kinase complex almost completely eliminated the accumulation of fibronectin in response to TGFβ (Fig. 3*D*).

Because Smad4 is a common mediator Smad for all TGFβ family pathways, we also examined the BMP pathway using the same set up in MDA-MB-468 cells. The BMP Smad1/5-specific promoter-reporter, BRE-luc, which is derived from the authentic SBE of the *Id1* gene enhancer (27), was activated by stimulation with BMP7 only after transfection of the cells with Smad4 (Fig. 3*E*). LSM co-expression decreased the transcriptional output of the promoter, similar to the effect LSM had on the TGFβ-specific reporter. Furthermore, the T77A Smad4 mutant again exhibited lower transcriptional activity in response to BMP7, as expected, and co-expression of LSM enzyme did not appreciably reduce the transcriptional output (Fig. 3*E*). At the endogenous gene level, we measured *Id1* mRNA expression and confirmed that BMP7 can induce *Id1* only in a Smad4-dependent manner; co-expression of LSM dramatically reduced the Smad4-dependent expression of the *Id1* gene (Fig. 3*F*). All of the above data therefore establish that LKB1 negatively regulates the DNA binding and the transcriptional activity of Smad4 as measured by transcriptional reporters and endogenous gene targets of the TGFβ and BMP pathways, for which Smad4 serves as an obligatory common signal transducer.

LKB1 and LIP1 Negatively Regulate TGFβ Signaling—The Smad4-dependent experiments suggested that LKB1 negatively regulates TGFβ and BMP signaling. In order to establish whether this is a more general property of the LKB1 signaling pathway, we performed both LKB1 gain-of-function and loss-of-function experiments and again measured pathway-specific transcriptional reporter activity and endogenous gene regulation.

In mouse pluripotent C2C12 myoblasts, TGFβ can induce robust levels of the *Pai-1* mRNA in a time-dependent manner (supplemental Fig. S3*A*). Transduction of the three LSM components into the C2C12 cells (for transduction efficiency, see supplemental Fig. S3, *B–D*) measurably reduced the levels of the *Pai-1* mRNA that accumulated at all time points (supple-

mental Fig. S3*A*). Using siRNA against endogenous LKB1, we could also confirm that knocking down LKB1 significantly enhanced the response of the Smad3/Smad4-specific CAGA-luc reporter (Fig. 4*A*). This was despite the fact that our siRNA reduced the endogenous LKB1 protein levels only down to 25% and not to zero (Fig. 4*A*). In the same line of evidence, LSM transduction into human hepatoma HepG2 cells reduced the activation of the CAGA-luc reporter by 70% (Fig. 4*B*). Similar results were obtained from additional cell types, as described below.

Because LIP1 also forms complexes with Smad4, we also examined whether LIP1 had negative effects similar to those of LKB1 on TGFβ and BMP signaling. Indeed, using a similar panel of cell models, we could demonstrate that depletion of endogenous LIP1 by means of siRNA enhanced TGFβ-dependent induction of the CAGA-luc reporter in stably transfected human fibrosarcoma HT-1080 cells (Fig. 4*C*). Transduction of human 293-T cells with the same shRNA vector targeting LIP1 as introduced in Fig. 1*E* and supplemental Fig. S1*B* led to enhanced BMP7-dependent induction of the BRE-luc reporter (Fig. 4*D*). Conversely, overexpression of LIP1 in the same experiment led to repression of the BMP7-inducible reporter activity and was sufficient to revert the enhanced reporter levels caused by the shRNA to those of control when silencing of endogenous LIP1 was combined with co-expression of exogenous LIP1 (Fig. 4*D*). In a similar manner, we could demonstrate a dose-dependent negative effect of LIP1 on the TGFβ-specific CAGA-luc (Fig. 4*E*) and on the BMP-specific BRE-luc (Fig. 4*F*) reporters in transfected HepG2 cells. It is worth noting that the effects of LIP1 depletion or overexpression on promoter-reporter activity were not as strong as those of LKB1 silencing or overexpression, which may reflect the fact that LIP1 is a scaffolding protein and its action toward the TGFβ and BMP pathways may depend either on endogenous LKB1 pools or on additional yet unknown endogenous factors. In agreement with this model, when low amounts of LIP1 and LKB1 were expressed in 293-T cells alone, they exhibited weak but significant inhibition of BMP signaling (now measured by means of the constitutively active mutant BMP-specific type I receptor ALK6QD) (Fig. 4*G*). When the same levels of LIP1 and LKB1 were co-expressed, a robust inhibition of BMP/ALK6 signaling was then observed by means of the transcriptional output of the BRE-luc reporter (Fig. 4*G*). These loss- and gain-of-function experiments therefore make apparent that LKB1 and LIP1 mediate negative control of TGFβ and BMP Smad signaling in a variety of cell types of different developmental origins.

LKB1 Promotes Epithelial Differentiation and Antagonizes TGFβ-induced EMT—As described in the Introduction, LKB1, via MARK signaling, is known to promote epithelial differentiation by inducing the assembly of the polarity complex (11). In contrast, TGFβ is a potent inducer of the EMT process in a variety of epithelial cell types (6). Based on the above evidence whereby LKB1 antagonizes TGFβ signaling, we reasoned that LKB1 might also block the EMT process in response to TGFβ. To examine this hypothesis, we used two well established cell models that respond to TGFβ and undergo EMT, human HaCaT keratinocytes (Fig. 5) and mouse
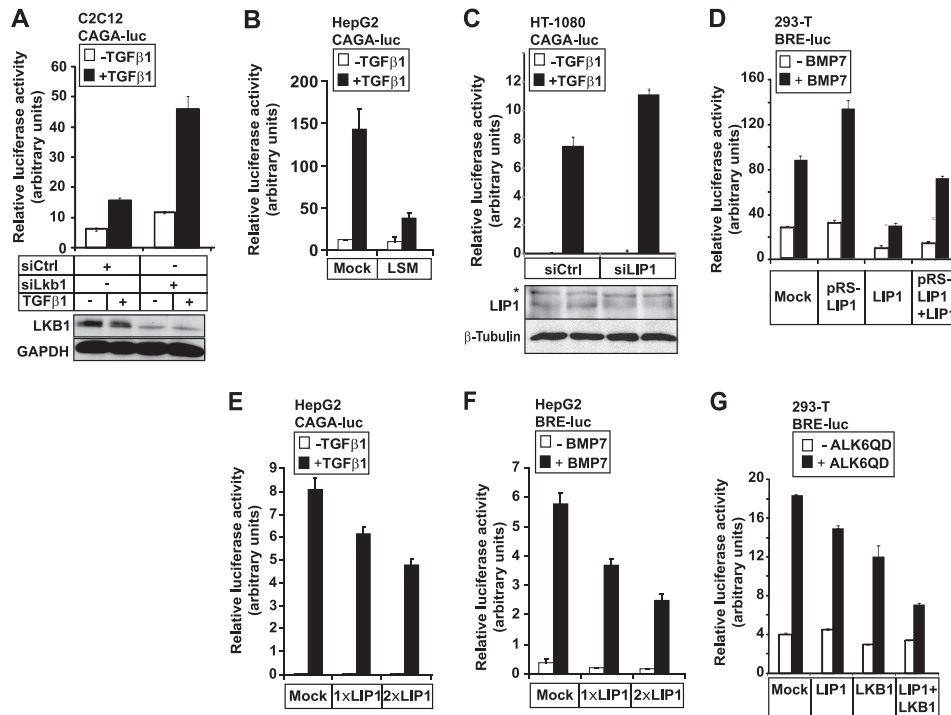
FIGURE 4. **LKB1 and LIP1 inhibit TGFβ and BMP signaling.** *A*, luciferase assay in C2C12 cells performed exactly as in Fig. 3*C* except that the cells were transfected with siRNA oligonucleotides against a nonspecific mRNA and the mouse-specific *Lkb1* mRNA. An immunoblot from the same transfected cells shows endogenous LKB1 and loading control GAPDH protein levels. *B*, luciferase assay in HepG2 cells performed as in Fig. 3*C*. *C*, luciferase assay in HT-1080 human fibrosarcoma cells stably expressing the same CAGA-luc reporter used in previous figures and after transient transfection with the control (*Ctrl*) and LIP1-specific siRNA and stimulation with 5 ng/ml TGFβ1 for 16 h. The data are presented as in Fig. 3*C*. An immunoblot from the same transfected cells shows endogenous LIP1 and loading control β-tubulin protein levels. An *asterisk* indicates a nonspecific protein band. *D*, luciferase assay in transfected 293-T cells with the BRE-luc reporter and the indicated constructs of pRS-LIP1 (shRNA vector) or pCDNA3-LIP1 (LIP1) after stimulation with 30 ng/ml BMP7 for 16 h. The data are presented as in Fig. 3*C*. *E*, luciferase assay in HepG2 cells performed as in Fig. 3*C*, except that the cells were transfected with the indicated mock and two doses of LIP1 vector DNA. *F*, luciferase assay in HepG2 cells performed as in *E*, except that the cells were transfected with the BRE-luc reporter and stimulated with 30 ng/ml BMP7. *G*, luciferase assay in 293-T cells performed as in *F*, except that the cells were transfected with the indicated vectors, and stimulation with BMP7 was replaced by co-transfection of the constitutively active ALK6 receptor mutant (ALK6QD). *Error bars*, S.D.

NMuMG breast epithelial cells (Fig. 6). During EMT, TGFβ induces the expression of the mesenchymal proteins PAI-1 and fibronectin, whereas the expression of the epithelial protein E-cadherin is down-regulated. Experiments in which endogenous LKB1 was knocked down to 10–20% of the control in HaCaT cells revealed enhanced (2-fold) induction of the mesenchymal PAI-1 and fibronectin markers and more efficient (2-fold) down-regulation of E-cadherin (Fig. 5, *A* and *B*). This was also observed microscopically because the HaCaT cells that were transduced with the LSM components appeared more compact and cuboidal and formed small clusters of cells with intense intercellular adhesion (Fig. 5*C*). Transduction with LSM also reduced TGFβ-induced endogenous fibronectin levels, indicating suppression of the EMT process. The same result was confirmed by visualizing the actin cytoskeleton of these epithelial cells (Fig. 5*D*). Upon TGFβ-induced EMT, the HaCaT actin cytoskeleton reorganizes, and thick stress fibers extend throughout the flattened and less adherent cells. Transduction with LSM blocked this effect to a great extent, and the actin cytoskeleton appeared as more compact cortical actin in the more cuboidal cells (Fig. 5*D*).

In order to link the mechanistic evidence of the action of LKB1 with the physiological effects measured during EMT, we also performed ChIP assays using a Smad4 antibody and analyzing binding of Smad4 to the regulatory sequences of the human *PAI-1* promoter (Fig. 5*E*). Whereas TGFβ stimulation

enhanced the binding of endogenous Smad4 to the *PAI-1* promoter sequences, transduction of the HaCaT cells with LSM reduced this TGFβ-inducible binding to the basal level (Fig. 5*E*). This result reflects faithfully the negative effect LKB1 exhibited during the *in vitro* DNA-binding assays (Fig. 3*A*). Finally, in the same line of evidence, LSM transduction into the HaCaT keratinocytes reduced the activation of the CAGA-luc reporter by 50% (Fig. 5*F*). We therefore conclude that in human HaCaT keratinocytes, LKB1 negatively regulates TGFβ-induced EMT by limiting Smad4-dependent transcriptional responses.

The same results were confirmed in the mouse NMuMG cells. After knockdown of endogenous LKB1 and TGFβ stimulation, the cells were clearly more elongated and mesenchymal-like than control cells in the presence of the nonspecific siRNA (Fig. 6*A*). EMT protein marker analysis also showed that the knockdown of endogenous LKB1 enhanced TGFβ-inducible levels of fibronectin (by 1.4-fold) and also led to a more robust down-regulation (by 1.3-fold) of E-cadherin levels (Fig. 6*B*). Inversely, transduction of NMuMG cells with LSM components led to reduced basal expression (by 4-fold) of fibronectin and reduced TGFβ-inducible fibronectin levels (by 1.4-fold) (Fig. 6*C*). In the same experiment, LSM transduction led to stronger basal E-cadherin levels (by 1.25-fold), which is compatible with the ability of LKB1 to promote epithelial differentiation (Fig. 6*C*). However, in this cell type,
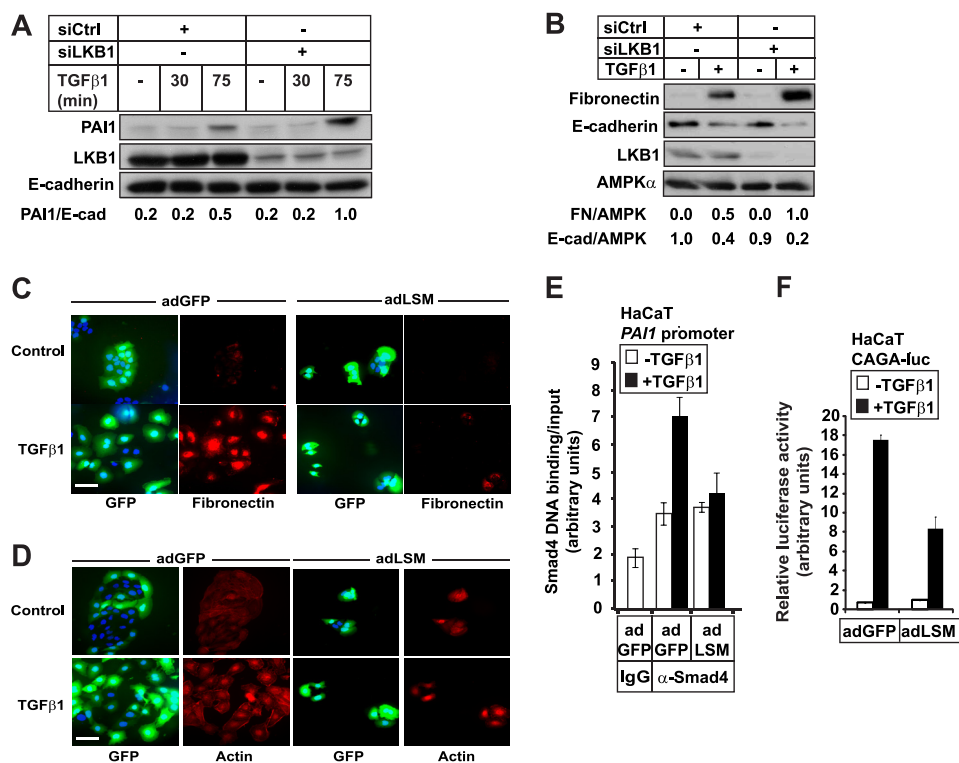
FIGURE 5. **LKB1 inhibits TGFβ-induced EMT in HaCaT keratinocytes.** *A,* immunoblot of the mesenchymal marker protein PAI-1, the epithelial marker protein E-cadherin and control LKB1 levels, in HaCaT cells transfected with the indicated siRNAs and stimulated with 5 ng/ml TGFβ1 for the indicated time periods. Note that at these early time points, the E-cadherin levels do not change and serve as loading controls. The protein levels of PAI-1 normalized to those of E-cadherin (*E-cad*) are plotted *below* the immunoblot. *B,* immunoblot from a similar experiment as in *A* except that the TGFβ1 stimulation lasted for 2 days. The AMPKα immunoblot serves as loading control. The protein levels of fibronectin (*FN*) or E-cadherin normalized to those of AMPKα are plotted *below* the immunoblot. *C,* immunofluorescence microscopy of HaCaT cells infected with the indicated adenoviral vectors and stimulated with 5 ng/ml TGFβ1 for 48 h. GFP autofluorescence indicates the infected cells as both control and LSM viruses encode for GFP. Endogenous fibronectin represents the mesenchymal marker analyzed. *Bar,* 10 μm. *D,* direct fluorescence microscopy of HaCaT cells prepared as in *C* and stained with phalloidin for their polymerized actin cytoskeleton. *Bar,* 10 μm. *E,* ChIP assay in HaCaT cells stimulated with TGFβ1 for 1.5 h using a control IgG or specific anti-Smad4 antibody, followed by real-time PCR for the *PAI-1* promoter sequence. Average values from triplicate determinations are plotted along with S.D. values (*error bars*). The ChIP analysis was repeated twice. *F,* luciferase assay in HaCaT cells performed as in Fig. 3C, except that the cells were infected with the indicated adenoviral vectors.

TGFβ was still capable of reducing significantly the E-cadherin protein levels (Fig. 6C). For this reason, we also analyzed E-cadherin mRNA levels (Fig. 6D) and found that silencing endogenous LKB1 led to a stronger (by 1.3-fold) down-regulation of E-cadherin mRNA by TGFβ, reflecting the protein data of Fig. 6B. In a similar manner, silencing endogenous LKB1 enhanced the TGFβ-induced fibronectin mRNA levels by 1.7-fold (Fig. 6E). In the same direction were the effects of LKB1 silencing on well established transcriptional repressors of E-cadherin, Snail1 and Slug (Fig. 6, F and G) (5). As previously established in NMuMG cells (29), TGFβ induced the mRNA levels of *Snail1* by 4-fold and, more weakly (1.4-fold), the levels of *Slug* (Fig. 6, F and G). After endogenous LKB1 silencing, the TGFβ-inducible levels of *Snail1* mRNA increased to 12-fold without major effects on its basal expression (Fig. 6F). In the same experiments, silencing LKB1 dramatically reduced *Slug* mRNA levels, whereas TGFβ could further induce this gene, in agreement with the rest of the data on EMT markers (Fig. 6G).

The process of EMT is known to correlate with increased invasiveness and metastasis of tumor cells (5). Because neither HaCaT nor NMuMG cells are tumorigenic, we employed human MDA-MB-231 breast carcinoma cells that are well studied in terms of their ability to metastasize in mouse xenografts

and also maintain TGFβ-dependent promigratory and proinvasive responses *in vitro* (30). In addition, MDA-MB-231 cells do not express endogenous LKB1 due to genetic deletion (31) and represent a good genetic model for LKB1 reconstitution. As previously established (30), we could measure a positive effect of TGFβ on the invasiveness of MDA-MB-231 cells transiently infected with control (GFP) adenovirus (Fig. 6H). When the cells were reconstituted with wild type human LKB1, the TGFβ-dependent effect on cell invasion through Matrigel was completely lost (Fig. 6H). This result is in full agreement with the effect of LKB1 on EMT of normal epithelial cells and with the general negative effect LKB1 exhibits over TGFβ signaling.

DISCUSSION

We provide the first clear evidence for a negative regulatory relationship between LKB1 and TGFβ family signaling. A second important negative regulator is the scaffolding protein LIP1 that binds to both LKB1 and to the common mediator Smad4 protein of the TGFβ and BMP pathways (Fig. 7A). LKB1 is capable of phosphorylating Thr[77] within the β-hairpin of the MH1 domain. The mechanism by which LKB1 negatively regulates TGFβ and BMP signaling involves negative regulation of Smad4 binding to DNA and reduced transcrip-
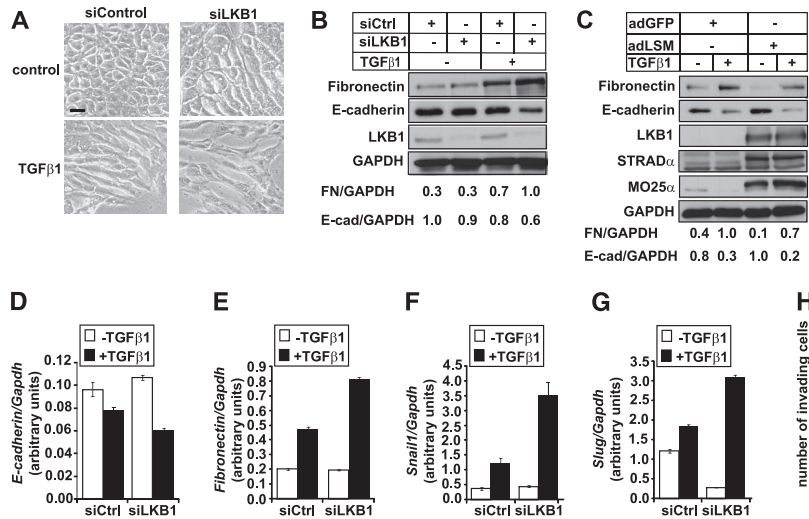
FIGURE 6. **LKB1 inhibits TGFβ-induced EMT in NMuMG breast epithelial cells.** *A*, phase-contrast microscopy of NMuMG cells transfected with the indicated siRNAs and stimulated with 5 ng/ml TGFβ1 for 24 h. *Bar*, 10 μm. *B*, immunoblot of the mesenchymal marker protein fibronectin, the epithelial marker protein E-cadherin, and control LKB1 and GAPDH levels in NMuMG cells transfected with the indicated siRNAs and stimulated with 5 ng/ml TGFβ1 for 24 h. The protein levels of fibronectin (*FN*) or E-cadherin (*E-cad*) normalized to those of GAPDH are plotted *below* the immunoblot. *C*, immunoblot from a similar experiment as in *B*, except that the cells were infected with the indicated adenoviral vectors and stimulated with 5 ng/ml TGFβ1 for 24 h. The protein levels of fibronectin or E-cadherin normalized to those of GAPDH are plotted *below* the immunoblot. A *star* indicates a nonspecific protein band. *D–G*, real-time RT-PCR analysis of the indicated mRNA levels normalized to the housekeeping *Gapdh* mRNA levels in NMuMG cells transfected with the indicated siRNAs and after stimulation with 5 ng/ml TGFβ1 for 48 h. Average relative expression values along with S.D. values (*error bars*) from triplicate determinations are plotted. Each experiment was repeated twice. *H*, transwell invasion assay of MDA-MB-231 cells into Matrigel after transient infection with the indicated adenoviruses, stimulation with 5 ng/ml TGFβ1 for 24 h, and counting of viable cells at the bottom side of the well. Average cell numbers from five sections of the well and corresponding S.D. values are plotted. Each invasion assay was performed twice.
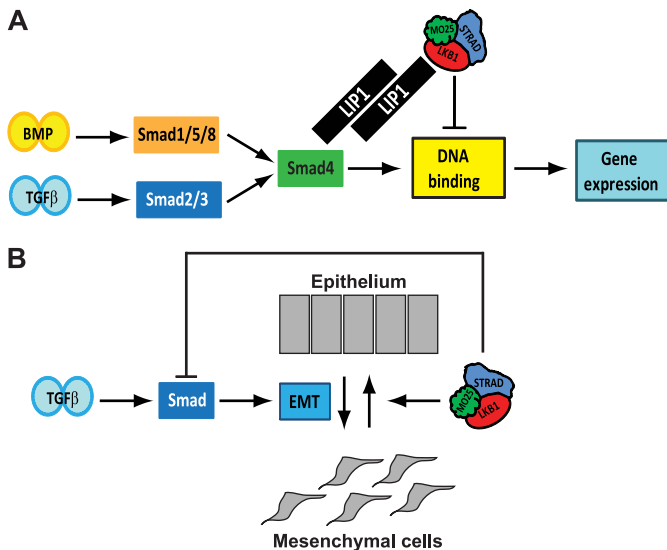

FIGURE 7. **LKB1 inhibits TGFβ/BMP signaling and EMT.** *A*, simplified signaling pathways of BMP and TGFβ, which are inhibited by LKB1 at the level of Smad4 binding to DNA. The complex of LIP1 with Smad4 and LKB1 is also shown. LIP1 is represented as a dimer based on the self-oligomerization data. *B*, TGFβ signaling promotes EMT. LKB1 promotes epithelial differentiation and also inhibits TGFβ signaling, which ensures inhibition of EMT.

tional activity of Smad4. Such negative regulation seems to involve many gene responses to TGFβ and BMP and has a clear impact on the process of EMT (Fig. 7*B*) and on tumor cell invasiveness. Thus, LKB1 promotes epithelial cell differentiation, whereas TGFβ signaling promotes mesenchymal transition (Fig. 7*B*).

The interaction between LIP1 and LKB1 and between LIP1 and Smad4 was previously characterized using cloned cDNA constructs (12). In this study, we demonstrate that endoge-

nous LIP1 is expressed in HaCaT cells and forms complexes with endogenous Smad4 (Fig. 1*D*) or endogenous LKB1 (Fig. 1*A*) and that shRNA-mediated silencing of LIP1 perturbs the ability of LKB1 to form complexes with Smad4 (Fig. 1*E*). In addition, complexes formed between endogenous LIP1 and endogenous LKB1 or overexpressed Smad4 could be observed (Fig. 1, *A* and *B*). These complexes were primarily constitutive and not dramatically affected by TGFβ or BMP receptor signaling (Fig. 1*G*). However, we failed to monitor detectable levels of endogenous LKB1-Smad4 complexes or the endogenous ternary complex of LKB1-LIP1-Smad4.[5] Although our molecular model would favor the formation of a ternary complex among these three proteins, the present data do not rigorously support such a model at the endogenous level. On the other hand, we were able to demonstrate that LIP1 is capable of forming homomeric complexes (Fig. 1*F*). This observation supports the notion that large protein complexes may occur with LIP1 homomers tethering in proximity LKB1 and Smad4 via independent LIP1 subunits (as hypothetically illustrated in Fig. 7*A*).

LIP1 is a rather large scaffolding protein with 1099 amino acid residues. It contains no obvious structural domains but has a glutamic acid- and leucine-rich repeat region (12). We have attempted to study more deeply the biological role of LIP1 in either LKB1 or TGFβ signaling and performed proteomic screens for the identification of new LIP1-interacting proteins (not shown). At this point, our efforts have not provided any solid evidence for a potent biological role of LIP1; however, the reported effects of LKB1 in regulating TGFβ signaling can to a certain extent involve the functional contribution of LIP1. Because LIP1 overexpression presented strong developmental phenotypes in *Xenopus* embryos (12), addi-

tional analysis of the biological functions of LIP1 are clearly warranted.

We demonstrate here for the first time that the LKB1 kinase can phosphorylate *in vitro* Smad4 on Thr[77] of its DNA-binding domain (Fig. 2) and in its linker domain (supplemental Fig. S2*B*). Despite a plethora of phosphorylation events described for R-Smads, such as Smad1, Smad2, and Smad3 (25), there is only a single previous report demonstrating specific phosphorylation of Smad4; this phosphorylation occurs in the linker domain and potentiates the transcriptional activity of Smad4 (26). Preliminary mutagenesis experiments have indicated that Thr[276] is not the linker phosphorylation site for LKB1.[5] The new site of Smad4 phosphorylation by LKB1 is functionally relevant because it is located close to the two major amino acid residues of the Smad4 MH1 domain β-hairpin that contact DNA directly (Fig. 2*E*). Our model therefore predicts that Smad4 phosphorylation by LKB1 affects binding of Smad4 to DNA, which was experimentally verified *in vitro* (Fig. 3, *A* and *B*) and via ChIP assays in intact cells (Fig. 5*E*). Whereas mutagenesis of Thr[77] to an alanine residue confirmed the specificity of the phosphorylation event (Fig. 2*D*), it also weakened significantly the DNA-binding and transcriptional activity of Smad4 (Fig. 3). This emphasizes that the site of Smad4 phosphorylation by LKB1 is a critical amino acid for the function of Smad4. Interestingly, the segment of the MH1 domain where Thr[77] resides is highly conserved among species (not shown) and between Smad family members (Fig. 2*E*). All human and mouse R-Smads have a serine in place of threonine. Furthermore, previous reports have established that the analogous serine residues in Smad2 (Ser[110]) and Smad3 (Ser[70]) are phosphorylated by different kinases, such as calmodulin kinase II and protein kinase C, respectively (32, 33). Phosphorylation of Smad3 on Ser[70] by protein kinase C was shown to inhibit binding to DNA, similar to the mechanism presented here for Smad4. Because LKB1 is capable of phosphorylating the MH1 domain of Smad3 at an as yet unidentified residue (supplemental Fig. S2*B*), it is possible that LKB1 plays a similar role as protein kinase C in controlling the function of Smad3, in addition to regulating Smad4. The exact physiological conditions under which LKB1 mediates phosphorylation of Smad4 (and Smad3) and a possible coordination of this mechanism with protein kinase C-mediated phosphorylation of Smad3 that could regulate the binding of the nuclear Smad complex to DNA remain to be elucidated.

In agreement with the effects LKB1 has on DNA binding of Smad4, we confirmed consistent negative regulation of TGFβ and BMP signaling by LKB1 (Figs. 3 and 4). This was demonstrated using artificial Smad-responsive promoter-reporter constructs and endogenous gene targets of TGFβ and BMP signaling. This finding is consistent with our previous demonstration that one of the kinases that is thought to act downstream of LKB1, the SIK1 kinase, also negatively regulates TGFβ signaling by down-regulating the TGFβ type I receptor (14). In this study, we have not examined whether the effects of LKB1 depend on any of the downstream kinases of the AMPK family that LKB1 is known to activate (7). The involvement of such kinases remains possible; however, the evidence of the LIP-Smad4 complex and the Smad4 phosphorylation

by LKB1 argues that LKB1 also has direct effects on Smad4 function.

We were unable to obtain evidence for a positive contribution of LKB1 to TGFβ or BMP signaling in any of the epithelial or mesenchymal progenitor cell types that we analyzed. This point is important because it has recently been reported that LKB1 is required for the secretion of TGFβ ligand by gastrointestinal and endothelial mouse cells, as demonstrated by knock-out of the *Lkb1* gene from these cell types (15, 17). More relevant to this study, *Lkb1* gene knock-out from mouse embryonic fibroblasts exhibited suboptimal TGFβ signaling, including transcriptional responses (16). Using a different source of *Lkb1* knock-out embryonic fibroblasts (34), we could confirm that indeed reconstitution of such cells with wild type LKB1 roughly doubled the response of endogenous TGFβ target genes, such as *Pai-1*.[5] Such results are in apparent contradiction to the negative regulation of TGFβ and BMP signaling demonstrated here. It is possible that this is due to the specific developmental origin of the embryonic fibroblasts and suggests that the role of LKB1 in regulating TGFβ pathways may be developmental stage-specific. Further research may provide new mechanistic explanations of this interesting but complex regulatory loop between LKB1 and TGFβ signaling.

Negative regulation of TGFβ signaling by LKB1 was finally confirmed using two independent cell models that undergo EMT in response to TGFβ (Figs. 5 and 6). Our original prediction was based on studies of the role of LKB1 during gastrointestinal epithelial polarity (11). According to this model, LKB1 positively regulates the assembly of the polarity complex that plays important roles in the establishment of the tight and adherens junctions. EMT does the opposite as it destroys epithelial differentiation and promotes a transition toward the mesenchymal cell lineage (5). Thus, it was logical to hypothesize that LKB1 would antagonize the EMT process, consistent with the evidence that LKB1 negatively regulates TGFβ signaling, a major pathway that promotes EMT (6). Based on the evidence that LKB1 negatively regulates the Smad4-dependent transcriptional induction of fibronectin in breast carcinoma MDA-MB-468 cells (Fig. 3*D*) and because fibronectin represents a well established mesenchymal marker protein, we argue that the effects of LKB1 on blocking EMT largely depend on its ability to negatively regulate Smad signaling. This was also corroborated by tumor cell invasion assays, where LKB1 neutralized the proinvasive effects of TGFβ without affecting significantly the basal invasive behavior of these cells that lack endogenous LKB1 (Fig. 6*H*). However, the independent effects that LKB1 has on polarity complex assembly (11) also argue that the antagonism of EMT by LKB1 may depend on additional mechanisms that center on the function of the polarity complex. This is highly possible because, in addition to the transcriptional mechanisms by which TGFβ induces EMT (3), a more direct signaling pathway is initiated by the TGFβ type II receptor kinase, which phosphorylates the Par6 component of the epithelial polarity complex and initiates ubiquitin-dependent degradation of key signaling proteins that regulate the assembly of tight junctions (35).

We therefore conclude that the transitions between epithelial and mesenchymal cells may be controlled by multiple balancing mechanisms that involve the activity of the LKB1 kinase on the one hand and of the TGFβ pathway on the other. These balancing mechanisms can possibly operate at the plasma membrane-proximal level of the polarity complex but also at the subsequent level of nuclear regulation of gene expression mediated by Smad proteins. The temporal aspects of such balanced regulation and the relative involvement of direct phosphorylation events mediated by LKB1 or the involvement of more indirect events mediated by downstream AMPK family members represent an exciting future area of research. The present paper sets the background stage for such explorations into the mechanisms of cross-talk between LKB1 and TGFβ signaling pathways and their impact in the process of EMT and tumor cell invasion.

REFERENCES

1. Feng, X. H., and Derynck, R. (2005) *Annu. Rev. Cell Dev. Biol.* **21,** 659–693
2. Lönn, P., Morén, A., Raja, E., Dahl, M., and Moustakas, A. (2009) *Cell Res.* **19,** 21–35
3. Moustakas, A., and Heldin, C. H. (2009) *Development* **136,** 3699–3714
4. Massagué, J. (2008) *Cell* **134,** 215–230
5. Thiery, J. P., Acloque, H., Huang, R. Y., and Nieto, M. A. (2009) *Cell* **139,** 871–890
6. Moustakas, A., and Heldin, C. H. (2007) *Cancer Sci.* **98,** 1512–1520
7. Alessi, D. R., Sakamoto, K., and Bayascas, J. R. (2006) *Annu. Rev. Biochem.* **75,** 137–163
8. Zeqiraj, E., Filippi, B. M., Deak, M., Alessi, D. R., and van Aalten, D. M. (2009) *Science* **326,** 1707–1711
9. Zeqiraj, E., Filippi, B. M., Goldie, S., Navratilova, I., Boudeau, J., Deak, M., Alessi, D. R., and van Aalten, D. M. (2009) *PLoS Biol.* **7,** e1000126
10. Tassan, J. P., and Le Goff, X. (2004) *Biol. Cell* **96,** 193–199
11. Baas, A. F., Boudeau, J., Sapkota, G. P., Smit, L., Medema, R., Morrice, N. A., Alessi, D. R., and Clevers, H. C. (2003) *EMBO J.* **22,** 3062–3072
12. Smith, D. P., Rayter, S. I., Niederlander, C., Spicer, J., Jones, C. M., and Ashworth, A. (2001) *Hum. Mol. Genet.* **10,** 2869–2877
13. Katoh, Y., Takemori, H., Horike, N., Doi, J., Muraoka, M., Min, L., and Okamoto, M. (2004) *Mol. Cell. Endocrinol.* **217,** 109–112
14. Kowanetz, M., Lönn, P., Vanlandewijck, M., Kowanetz, K., Heldin, C. H., and Moustakas, A. (2008) *J. Cell Biol.* **182,** 655–662
15. Katajisto, P., Vaahtomeri, K., Ekman, N., Ventelä, E., Ristimäki, A., Bardeesy, N., Feil, R., DePinho, R. A., and Mäkelä, T. P. (2008) *Nat. Genet.* **40,** 455–459
16. Vaahtomeri, K., Ventelä, E., Laajanen, K., Katajisto, P., Wipff, P. J., Hinz, B., Vallenius, T., Tiainen, M., and Mäkelä, T. P. (2008) *J. Cell Sci.* **121,** 3531–3540
17. Londesborough, A., Vaahtomeri, K., Tiainen, M., Katajisto, P., Ekman, N., Vallenius, T., and Mäkelä, T. P. (2008) *Development* **135,** 2331–2338
18. Morén, A., Hellman, U., Inada, Y., Imamura, T., Heldin, C. H., and Moustakas, A. (2003) *J. Biol. Chem.* **278,** 33571–33582
19. Kowanetz, M., Valcourt, U., Bergström, R., Heldin, C. H., and Moustakas, A. (2004) *Mol. Cell. Biol.* **24,** 4241–4254
20. Noga, A. A., Soltys, C. L., Barr, A. J., Kovacic, S., Lopaschuk, G. D., and Dyck, J. R. (2007) *Am. J. Physiol. Heart Circ. Physiol.* **292,** H1460–H1469
21. Kurisaki, A., Kose, S., Yoneda, Y., Heldin, C. H., and Moustakas, A. (2001) *Mol. Biol. Cell* **12,** 1079–1091
22. Berns, K., Hijmans, E. M., Mullenders, J., Brummelkamp, T. R., Velds, A., Heimerikx, M., Kerkhoven, R. M., Madiredjo, M., Nijkamp, W., Weigelt, B., Agami, R., Ge, W., Cavet, G., Linsley, P. S., Beijersbergen, R. L., and Bernards, R. (2004) *Nature* **428,** 431–437
23. Jurek, A., Amagasaki, K., Gembarska, A., Heldin, C. H., and Lennartsson, J. (2009) *J. Biol. Chem.* **284,** 4626–4634
24. Morén, A., Itoh, S., Moustakas, A., Dijke, P., and Heldin, C. H. (2000) *Oncogene* **19,** 4396–4404
25. Wrighton, K. H., Lin, X., and Feng, X. H. (2009) *Cell Res* **19,** 8–20
26. Roelen, B. A., Cohen, O. S., Raychowdhury, M. K., Chadee, D. N., Zhang, Y., Kyriakis, J. M., Alessandrini, A. A., and Lin, H. Y. (2003) *Am. J. Physiol. Cell Physiol.* **285,** C823–C830
27. Korchynskyi, O., and ten Dijke, P. (2002) *J. Biol. Chem.* **277,** 4883–4891
28. Dennler, S., Itoh, S., Vivien, D., ten Dijke, P., Huet, S., and Gauthier, J. M. (1998) *EMBO J.* **17,** 3091–3100
29. Thuault, S., Valcourt, U., Petersen, M., Manfioletti, G., Heldin, C. H., and Moustakas, A. (2006) *J. Cell Biol.* **174,** 175–183
30. Deckers, M., van Dinther, M., Buijs, J., Que, I., Löwik, C., van der Pluijm, G., and ten Dijke, P. (2006) *Cancer Res.* **66,** 2202–2209
31. Shen, Z., Wu, Q., Yue, L., Li, H. C., Shen, Z. Z., and Shao, Z. M. (2005) *Zhonghua Yi Xue Za Zhi* **85,** 15–18
32. Wicks, S. J., Lui, S., Abdel-Wahab, N., Mason, R. M., and Chantry, A. (2000) *Mol. Cell. Biol.* **20,** 8103–8111
33. Yakymovych, I., Ten Dijke, P., Heldin, C. H., and Souchelnytskyi, S. (2001) *FASEB J.* **15,** 553–555
34. Bardeesy, N., Sinha, M., Hezel, A. F., Signoretti, S., Hathaway, N. A., Sharpless, N. E., Loda, M., Carrasco, D. R., and DePinho, R. A. (2002) *Nature* **419,** 162–167
35. Ozdamar, B., Bose, R., Barrios-Rodiles, M., Wang, H. R., Zhang, Y., and Wrana, J. L. (2005) *Science* **307,** 1603–1609